The junctional SR protein JP-45 affects the functional expression of the voltage-dependent Ca^{2+} channel $Ca_v1.1$

Ayuk A. Anderson[1], Xavier Altafaj[2], Zhenlin Zheng[3], Zhong-Min Wang[3], Osvaldo Delbono[3,4], Michel Ronjat[2], Susan Treves[1] and Francesco Zorzato[5,*]

[1]Departments of Anaesthesia and Research, Basel University Hospital, Hebelstrasse 20, 4031 Basel, Switzerland
[2]INSERM U607/CEA/UJF, Lab CCFP/DRDC, Rue des Martyrs 17, 38054, Grenoble, Cedex 9 France
[3]Department of Physiology and Pharmacology and [4]Department of Internal Medicine, Gerontology, Wake Forest University School of Medicine, Winston-Salem, NC 27157, USA
[5]Department of Experimental and Diagnostic Medicine, General Pathology Section, University of Ferrara, Via Borsari 46, 44100 Ferrara, Italy
*Author for correspondence (e-mail: zor@unife.it)

Accepted 14 February 2006
Journal of Cell Science 119, 2145-2155 Published by The Company of Biologists 2006
doi:10.1242/jcs.02935

Summary

JP-45, an integral protein of the junctional face membrane of the skeletal muscle sarcoplasmic reticulum (SR), colocalizes with its Ca^{2+}-release channel (the ryanodine receptor), and interacts with calsequestrin and the skeletal-muscle dihydropyridine receptor Ca_v1. We have identified the domains of JP-45 and the $Ca_v1.1$ involved in this interaction, and investigated the functional effect of JP-45. The cytoplasmic domain of JP-45, comprising residues 1-80, interacts with $Ca_v1.1$. JP-45 interacts with two distinct and functionally relevant domains of $Ca_v1.1$, the I-II loop and the C-terminal region. Interaction between JP-45 and the I-II loop occurs through the α-interacting domain in the I-II loop. β1a, a Ca_v1 subunit, also interacts with the cytosolic domain of JP-45, and its presence drastically reduces the interaction between JP-45 and the I-II loop. The functional effect of JP-45 on $Ca_v1.1$ activity was assessed by investigating charge movement in differentiated C2C12 myotubes after overexpression or depletion of JP-45. Overexpression of JP-45 decreased peak charge-movement and shifted $V_{Q1/2}$ to a more negative potential (–10 mV). JP-45 depletion decreased both the content of $Ca_v1.1$ and peak charge-movements. Our data demonstrate that JP-45 is an important protein for functional expression of voltage-dependent Ca^{2+} channels.

Key words: Voltage-dependent Ca^{2+} channel, JP-45, Sarcoplasmic reticulum, Excitation-contraction coupling

Introduction

The sarcoplasmic reticulum (SR) of the skeletal muscle and the transverse tubular membranes provide a conducive environment enriched with key proteins that have been shown to play an essential role in excitation-contraction (E-C) coupling (Endo, 1977; Fleischer and Inui, 1989). E-C coupling occurs in specialized junctions called triads, which are an intracellular synapse formed by the membrane system of the transverse tubule and the terminal cisternae of the SR. The two main Ca^{2+} channels involved in E-C coupling are the dihydropyridine receptor, Ca_v1, which lies on the transverse tubules where it acts as a voltage sensor for E-C coupling, and the ryanodine receptor (RyR), present on the junctional face membrane of the SR, which is the Ca^{2+} release channel (Franzini-Armstrong and Jorgensen, 1994; Meissner, 1994; Ma and Pan, 2003; Sutko and Airey, 1996; Franzini-Armstrong, 1980; Lamb and Stephenson, 1990; Rios and Pizzarro, 1991). Ca_v1 is a hetero-oligomeric complex made up of at least four subunits: α1, β, $\alpha_2\delta$ and γ (Leung et al., 1987; Lacerda et al., 1991; Birnbaumer et al., 1998; Catterall, 1995; Snutch and Reiner, 1992). The pore-forming $Ca_v1.1$ is an integral membrane protein and is indispensable for E-C coupling, whereas the cytosolic β1a and $\alpha_2\delta$ subunits have regulatory functions; the role of the γ subunit has yet to be clearly defined (Catterall, 1995; Snutch and Reiner, 1992, Tsien et al., 1991). The β1a subunit associates tightly with the $Ca_v1.1$ by binding to a region on the I-II loop termed α-interacting domain (AID) (Pragnell et al., 1994). The β1a subunit is important for plasma membrane expression of the $Ca_v1.1$, whereas a sequence located in the C-terminal domain of the $Ca_v1.1$ seems to be involved in triad targeting (Chien et al., 1995; Flucher et al., 2000; Flucher et al., 2002), although other domains and/or polypeptides might be involved in proper targeting.

In skeletal muscle, $Ca_v1.1$ responds to transverse tubule depolarisation by sensing the voltage change and it induces Ca^{2+} release from the SR through a direct interaction with the RyR. Besides the RyR, however, the junctional face membrane contains numerous other proteins that, because of their anatomical location, are deemed to be involved in E-C coupling (Zhang et al., 1997; Costello et al., 1986; Zorzato et al., 2000). In the past few years a number of investigators have begun to define the major and minor structural components of the junctional face membrane (Ito et al., 2001; Takeshima et al., 2000). In previous studies (Zorzato et al., 2000; Anderson et al., 2003), we identified and characterized – at the biochemical and molecular level – JP-45, an integral membrane protein

constituent of the SR junctional face membrane in skeletal muscle. We also showed that JP-45 colocalizes with the RyR Ca^{2+}-release channel and interacts with $Ca_v1.1$ and the luminal Ca^{2+}-binding protein calsequestrin (Anderson et al., 2003). To gather insight into the functional role of JP-45, we defined the domains involved in the interaction between JP-45 and $Ca_v1.1$. Our results demonstrate that the cytoplasmic domain of JP-45 interacts directly with the I-II loop, the C-terminal domain of $Ca_v1.1$ subunit and also with the β1a subunit of Ca_v1. In addition, we show that the interaction between JP-45 and the I-II loop occurs through the AID domain, and can be displaced by β1a. Experimental evidence has demonstrated that the β1a subunit interacts with the $Ca_v1.1$ subunit via AID (Pragnell et al., 1994; Chen et al., 2004) and that this protein-protein interaction is involved in the insertion of the voltage sensor to its proper membrane compartment (Flucher et al., 2002). To confirm the functional role of JP-45 in vivo, we overexpressed and silenced endogenous JP-45 in C2C12 cells and studied their electrophysiological properties. Based on the results of the present report, JP-45 is involved in the regulation of the functional expression of $Ca_v1.1$ into the transverse tubular membrane compartment.

Results and Discussion

Identification of domains enabling the interaction of JP-45 and $Ca_v1.1$

In a previous report, we demonstrated that JP-45 interacts with native $Ca_v1.1$ (Anderson et al., 2003). Here, we describe a series of experiments to identify the domains participating in this interaction. We prepared recombinant GST-fusion proteins covering different coding regions of JP-45 (excluding the transmembrane domain) (see Fig. 1). These proteins were then bound to glutathione-Sepharose beads and incubated with solubilized light microsomal vesicles. Fig. 2A shows that the cytoplasmic N-domain of JP-45, more specifically the region between residues 1-80 (domain 2) interacts with native $Ca_v1.1$. No interaction was observed between any other JP-45 domains and $Ca_v1.1$. The physiological relevance of the interaction of fusion proteins was verified by studying the effect of the GST-JP-45 domain 2 on co-immunoprecipitation of $Ca_v1.1$ with a monoclonal anti-JP-45 antibody (Ab). The interaction between native JP-45 and $Ca_v1.1$ was competed-out by the presence of soluble GST-JP-45 domain 2 in the co-immunoprecipitation reaction (Fig. 2B).

Extensive structure-to-function relationship studies on Ca_v1 have helped to define functionally relevant domain boundaries not only among the subunits making up the supramolecular complex, but also within the primary structure of each subunit (Nakai et al., 1998; Grabner et al., 1999; Kugler et al., 2004; Van Petegem et al., 2004). We reasoned that the physiological relevance of the interaction between $Ca_v1.1$ and JP-45 could be better understood if we first identified JP-45-binding sites within the $Ca_v1.1$. GST-JP-45 domain-2 fusion protein was immobilized on GST-Sepharose and incubated with different His-tagged fusion proteins, covering the cytoplasmic domains of the $Ca_v1.1$ subunit (Tanabe et al., 1987). Whereas some of the His-tagged fusion proteins display the expected molecular mass, they had in other cases a molecular mass lower than the expected value due to the instability of purified fusion proteins (Fig. 3A, lanes 3 and 7). The protein-protein-interaction experiments depicted in Fig. 3B demonstrate that the I-II loop and the C-terminal domain of the $Ca_v1.1$ as well as the β1a subunit interact with JP-45, whereas fusion proteins corresponding to the N-terminus – the II-III and III-IV loops of the $Ca_v1.1$ subunit – do not interact with GST-JP-45 domain-2 fusion protein. To validate these results, we performed pull-down experiments using GST-JP-45 domain 2 as bait and solubilized light microsomal vesicles as ligand, in the presence or absence of increasing concentrations of either I-II loop or recombinant C-terminal-distal His-tag fusion proteins. Inhibition of $Ca_v1.1$-GST-JP-45 interaction was achieved at 3.6 and 1.25 μM of I-II loop and C-terminal-distal His-tag fusion proteins, respectively. To further confirm the specificity of the pull-down assay, we also investigated these interactions under native conditions, i.e. by performing co-immunoprecipitation of native JP-45 with $Ca_v1.1$ using the monoclonal anti-JP-45 Ab, in the presence or absence of competing I-II loop or recombinant C-terminal-distal His-tag fusion proteins. As shown in Fig. 3D, the presence of the competing recombinant fusion proteins substantially diminished the interaction between JP-45 and the $Ca_v1.1$ domains. Pull-down and co-immunoprecipitation assays demonstrated that competition with one of the $Ca_v1.1$ interacting domains (I-II loop or C-terminal-distal His-tag fusion proteins) was sufficient to partially inhibit the interaction. At a first glance it seems unclear how preventing the $Ca_v1.1$–JP-45 interaction through a single domain reduces total binding to the $Ca_v1.1$ to almost zero. A plausible explanation of the experiments is described in Fig. 3C and D; addition of excess I-II loop or C-terminal-distal loop occupies the interacting domain of the N-terminal domain of JP-45. Binding of the 50 aa-long JP-45 binding sites by an excess of the 14 kDa or 30 kDa $Ca_v1.1$ loops (I-II and C-terminal, respectively) most probably creates a steric hindrance, whereby the interaction of alternative domains within the native solubilized $Ca_v1.1$ is either abolished or substantially weakened.

Immunoprecipitation experiments revealed that JP-45

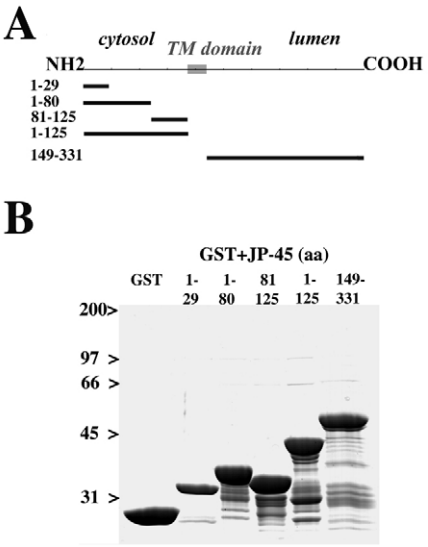

Fig. 1. Domains of JP-45 used to identify the $Ca_v1.1$ binding sites. (A) Schematic representation. (B) 10% SDS-PAGE and Coomassie Brilliant Blue staining of the GST-JP-45 fusion proteins purified by glutathione-Sepharose. The numbers above each lane indicate the aa residues that were fused in frame in the pGex plasmid to yield the GST-JP-45 fusion protein.

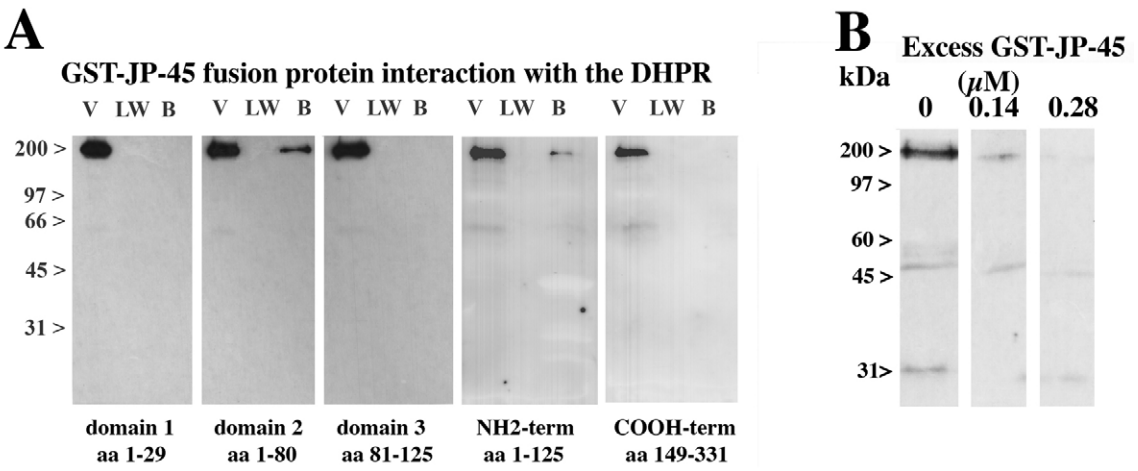

Fig. 2. Identification of the JP-45 domain interacting with $Ca_v1.1$. (A) GST-JP-45 fusion proteins encompassing different domains of JP-45 were bound to glutathione-Sepharose beads and incubated with solubilized rabbit skeletal-muscle microsomal vescicles as described in Materials and Methods. Proteins present in the void (V), last wash (LW) and bound to the beads (B) were separated on a 10% SDS-PAGE, transferred onto nitrocellulose and the presence of the bound $Ca_v1.1$ was revealed by western blotting with commercial anti-$Ca_v1.1$ Abs. (B) Co-immunoprecipitation experiment with monoclonal anti-JP-45 Ab to pull-down $Ca_v1.1$. Experiments were performed as described in the Materials and Methods. Where indicated, recombinant GST-JP-45 domain-2 fusion protein was used to compete-out the interaction between endogenous proteins present in the microsomes forming a supramolecular complex.

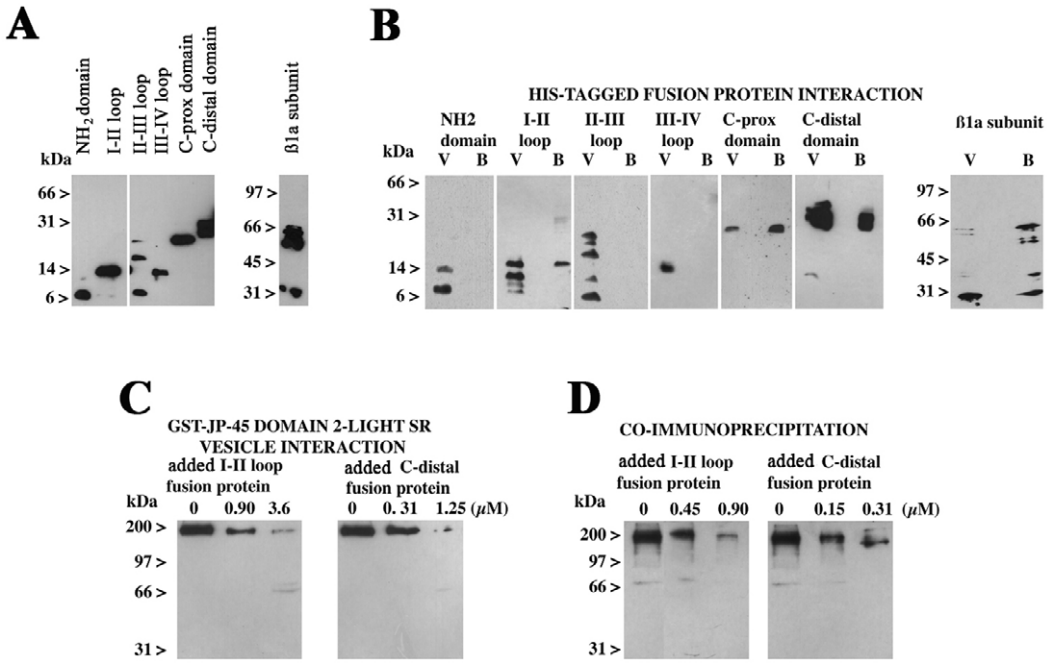

Fig. 3. Identification of $Ca_v1.1$ domains interacting with JP-45. $Ca_v1.1$ domains I-II, C-terminal-distal and C-terminal-proximal His-tag fusion proteins, and subunit β1a interact with the cytosolic domain of JP-45. (A) Immunoblot of purified His-tagged fusion proteins encompassing the different $Ca_v1.1$ domains (10% tricine SDS-PAGE) and β1a (10% SDS-PAGE). Immunostaining was carried out using commercial anti-poly-His Abs followed by HR-conjugated anti-mouse IgG; bands were visualized by chemiluminescence. (B) Pull-down of His-tagged fusion proteins with domain 2 of JP-45 (aa residues 1-80). GST-JP-45 domain-2 fusion protein was bound to glutathione-Sepharose beads and incubated with the His-tagged recombinant $Ca_v1.1$ proteins. Proteins present in the void (V) or bound to the beads (B) were separated on a 10% tricine SDS-PAGE or 10% SDS-PAGE (for the β1a subunit), blotted onto nitrocellulose and visualized in western blots by using anti-poly-His Ab as described above. (C) GST-JP-45 domain-2 fusion protein was bound to glutathione-Sepharose beads and incubated with solubilized light SR vescicles isolated from rabbit skeletal muscle in the presence of the indicated concentration of competing His-tagged I-II loop or C-terminal-distal His-tag fusion proteins. (D) Monoclonal anti-JP-45 Abs were used to co-immunoprecipitate the complex from solubilized light microsomal vescicles isolated from rabbit skeletal muscle in the presence of the indicated concentration of competing His-tagged I-II loop or C-terminal-distal fusion proteins. Proteins bound to the beads were separated in a 10% SDS-PAGE, transferred onto nitrocellulose and probed with anti-$Ca_v1.1$ Abs.

interacts with the I-II loop of subunit $Ca_v1.1$ and with purified recombinant β1a subunit (Fig. 3B). The β1a has been shown to interact strongly with the I-II loop of the α1.1 subunit and to affect its functional expression (Flucher et al., 2000; Chien et al., 1995). In the next set of experiments, we therefore characterized in greater detail the latter protein-protein interaction.

Effect of the β1a subunit on the interaction of JP-45 and $Ca_v1.1$

We investigated the role of the β1a subunit on the interaction between JP-45 and $Ca_v1.1$ by pull-down and co-immunoprecipitation assays (Fig. 4). JP-45 domain-2 fusion protein was immobilized on GST-Sepharose and incubated with the His-tagged $Ca_v1.1$ subunit I-II loop fusion protein in the presence or absence of increasing concentrations of β 1a fusion protein. As seen in Fig. 4A the presence of β1a interferes with the interaction between the I-II loop and JP-45. Pull-down assays were also performed by using the solubilized light microsomal vesicles as ligand. In the latter case, the association between the GST-JP-45 domain-2 fusion protein and the native $Ca_v1.1$ subunit was remarkably weaker in the presence of excess β1a-His-tagged fusion protein (Fig. 4B). The interference of the interaction between JP-45 and the $Ca_v1.1$ subunit by excess β1a, was also confirmed by performing co-immunoprecipitation experiments with anti-JP-45 Abs to pull-down the native solubilized complex (Fig. 4C). These results suggest that the presence of excess β1a disrupts the complex between $Ca_v1.1$ and JP-45. We cannot discriminate whether JP-45 interacts with the $Ca_v1.1$ or β1a, subunit, or whether JP-45 interacts with both subunits, thereby forming an oligomeric complex.

The Ca_v1 β1a subunit has been shown to bind strongly to the intracellular loop between transmembrane domain I and II of the $Ca_v1.1$, a region composed of 18 aa displaying the motif QQ-E-L-GY-WI-E, conserved in different isoforms (Pragnell et al., 1994). This binding domain is also referred to as α-interacting domain (AID). It is thought that the interaction between AID and the β1a subunit is important to determine the stability of this Ca^{2+} channel on the plasma membrane (Birnbaumer et al., 1998; Flucher et al., 2000; Flucher et al., 2002; Chien et al., 1995; Ahern et al., 2003; Bichet et al., 2000). In addition, the interaction between AID and β1a is regarded to the major structural determinant required for the surface expression of $Ca_v1.1$ (Chien et al., 1995; Beurg et al., 1999; Gregg et al., 1996; Jones et al., 1998). Coexpression of $Ca_v1.1$ and β1a subunits has been shown to increase the density and kinetics of L-type Ca^{2+} currents, and experimental evidence suggest that the β1a subunit facilitates gating of $Ca_v1.1$ by increasing the coupling between charge movement and pore opening (Sheridan et al., 2003; Sheridan et al., 2004). These effects of the β1a subunit are due to its interaction with the I-II loop, a domain that also interacts with JP-45. In the next set of experiments we addressed the question of whether the β1a subunit and JP-45 share the AID domain as binding site on the I-II loop. To address this issue, we performed pull-down assays with (1) GST-I-II loop fusion protein, (2) with a GST-fusion protein containing AID flanked by 21 and 11 residues at the N-terminal and C-terminal end, respectively, and (3) with a synthetic biotinylated-AID peptide. For the first two assays, the GST-fusion proteins were used as bait and the His-tagged JP-45 domain-2 fusion protein as ligand. The apparent molecular mass of His-tagged JP-45 domain 2 is

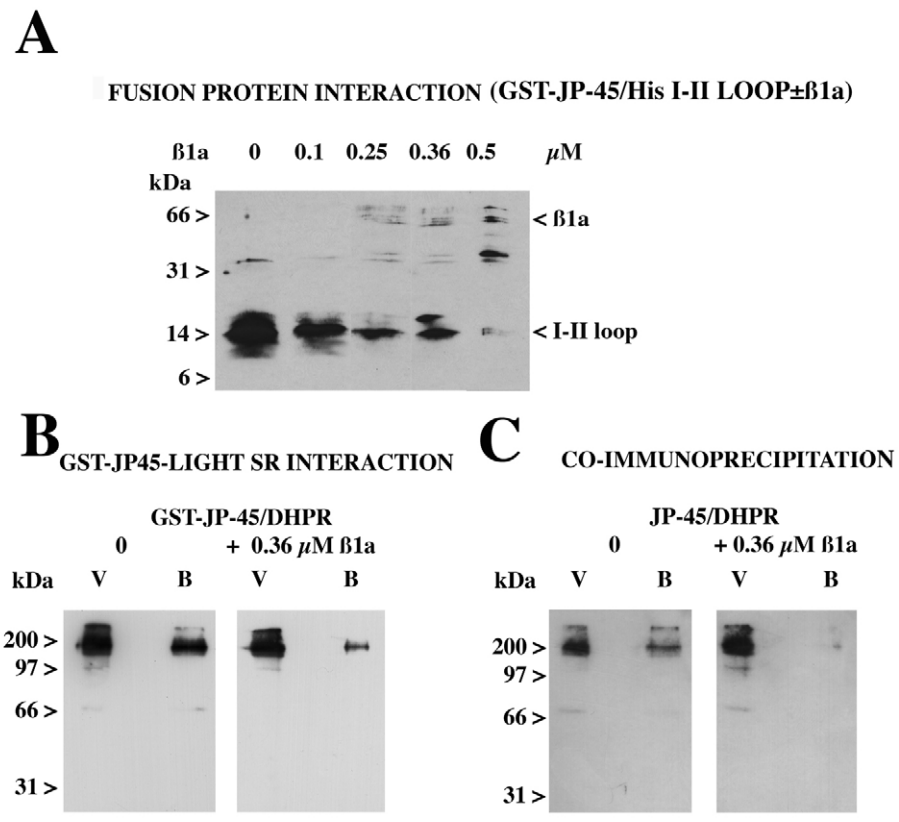

Fig. 4. Effect of the β1a subunit on the interaction between JP-45 and $Ca_v1.1$. (A) Interaction between GST-JP-45 and His I-II loop in the presence of competing purified β1a subunit. For the fusion-protein–protein interaction, 0.57 μM of GST-JP-45 domain 2 and 1.4 μM I-II loop fusion protein were incubated in the presence of the indicated concentration of His-tagged β1a subunit. His-tagged I-II loop fusion proteins bound to glutathione-Sepharose beads coated with GST-JP-45 domain-2 fusion protein were separated on a 10% tricine SDS-PAGE and probed with anti-poly-His Ab as described in the legend to Fig. 3. (B) Solubilized rabbit skeletal-muscle light SR vesicles were incubated with glutathione-Sepharose beads coated with GST-JP-45 domain-2 fusion protein in the absence or presence of purified β1a subunit. Proteins present in the void (V) and bound to the beads (B), were separated on a 10% SDS-PAGE, blotted onto nitrocellulose and probed with anti-α1.1 subunit Ab. (C) Solubilized rabbit skeletal-muscle light SR vesicles were incubated with anti-JP-45 Ab followed by incubation with Sepharose-protein G beads in the absence or presence of competing purified β1a subunit. Proteins present in the void (V) and bound to the beads (B), were separated on a 10% SDS-PAGE, blotted onto nitrocellulose and probed with anti-$Ca_v1.1$ Ab.

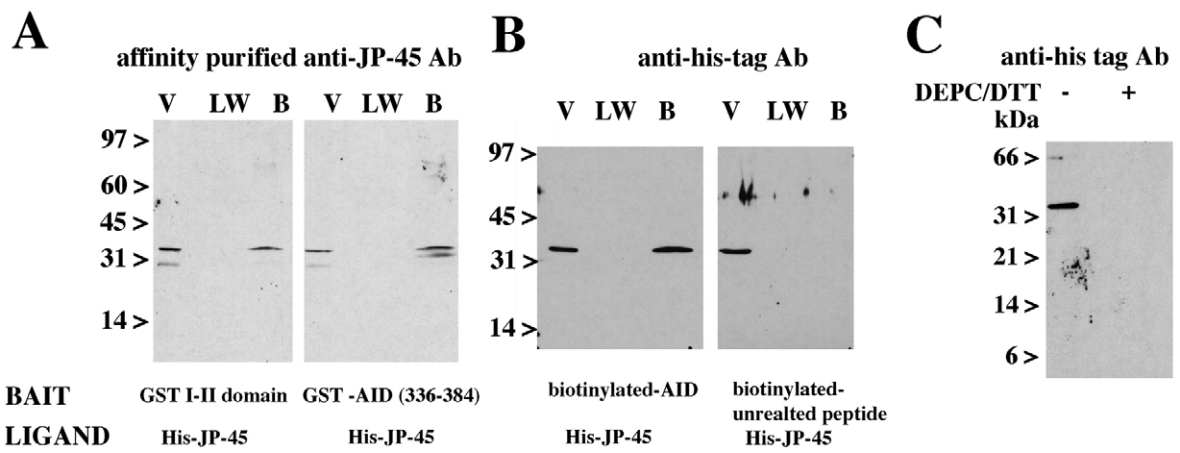

Fig. 5. JP-45 interacts with the AID domain on the I-II loop of $Ca_v1.1$. (A) GST-I-II loop fusion protein or the GST-AID containing domain encompassed within $Ca_v1.1$ residues 336-384 were incubated with His-tagged JP-45 domain-2 fusion protein. Pull-down was performed as described in Fig. 3; proteins in the void (V), last wash (LW) or bound to the glutathione resin (B) were separated on a 12.5% SDS-PAGE, transferred onto nitrocellulose and probed with affinity-purified anti-JP-45 Ab. (B) Synthetic biotinylated peptides corresponding to the AID sequence or an unrelated biotinylated peptide were used to coat neutroavidine beads, which were subsequently incubated with His-JP-45 domain 2. Proteins present in the void, last wash or bound to the beads were separated on a 12.5% SDS-PAGE, transferred onto nitrocellulose and the immunopositive band was visualized using anti-His-tag commercial Abs. (C) A His-tagged fusion protein encompassing domain 2 JP-45 was prepared as described in Materials and Methods. Although the fusion protein migrated slower in SDS-PAGE, its identity was verified by direct sequencing (not shown) and by immunoblotting with anti-His Ab. Note that treatment of the fusion protein with DTT+DEPC eliminated its immunoreactivity.

larger than the theoretical predicted values (approx. 31 kDa vs 14 kDa, respectively). We are confident that the apparent larger molecular mass of the His-tagged JP-45 domain-2 fusion protein is due its dimerization, because its treatment with DEPC (which destroys the His tag) abolished the binding of the anti-His tag Ab (Fig. 5 panel C). Western blot analysis (Fig. 5A,B) demonstrates that JP-45 domain 2 interacts directly with the AID sequence within the I-II loop. The in vitro interaction of the sequence containing AID and JP-45 occurs at micromolar concentrations of His-tagged JP-45 domain-2 fusion protein. Because of such a high concentration it is probably that, under physiological conditions, the interaction between the β1a subunit and AID prevails over that of JP-45 and AID. Nevertheless, on the basis of the highly organized molecular assembly of the triad membranes, we cannot exclude the possibility that the local concentration of JP-45 in the triadic gap is sufficient to interfere either with the high-affinity interaction between AID and the β1a subunit (Pragnell et al., 1994; Sheridan et al., 2003; Strube et al., 1996). If there are no other proteins involved in the interaction with AID, our data imply that, in the β1a subunit knock-out animal, AID is occupied mainly by JP-45 and that such an interaction might account, at least in part, for the severe phenotype of the mice (Gregg et al., 1996). Strube et al. have shown that mouse skeletal muscle cells with a null-mutation in the *cchb1* gene (encoding the β1a subunit of the Ca_v1) show a significant decrease in maximum charge-movement and a shift in the half-activation potential towards more negative potentials (Strube et al., 1996).

To investigate the functional effect of JP-45, we altered the stoichiometry of the JP-45–$Ca_v1.1$ supramolecular complex either by JP-45 overexpression or by JP-45 gene silencing in differentiated C2C12 myotubes, and then examined $Ca_v1.1$ activity by measuring charge movement.

Effect of JP-45–DsRed2 overexpression on the function of the $Ca_v1.1$

To examine the expression of JP45 and the $Ca_v1.1$, we carried out western blot analysis on subcellular fractions isolated from transfected cells. Fig. 6A shows a western blot of total microsome fractions from C2C12 cells transfected either with pFP-N3 coupled to red fluorescent protein (DsRed2) (pFP-N3–DsRed2) vector or with JP-45–pFP-N3–DsRed2 plasmid. Cells transfected with the latter plasmid show an immunoreactive band of approximately 45 kDa, which represents endogenous JP-45, and a band of approximately 70 kDa, which represents the JP-45-DsRed fusion protein. To verify whether overexpression of JP-45 affects the average amount of $Ca_v1.1$ subunit, we performed immunoprecipitation experiments. Total C2C12 lysate of control and JP45-overexpressing cells contain two distinct high-molecular mass bands of 175 kDa and 170 kDa that can be attributed to the $Ca_v1.1$ subunit (Leung et al., 1987). The relative amount of protein in the bands did not show a major change (intensity ratio of $Ca_v1.1$ bands in JP45-overexpressing cells to those of cells expressing empty vector was 0.971±0.06, mean ± s.d.). C2C12 cells were transfected with JP-45–pFP-N3–DsRed2 and the expression of JP-45–DsRed2 fusion protein was monitored by fluorescence microscopy to measure direct charge-movement. Fig. 7A shows the maximal charge movement. Fluorescence relationship for C2C12 cells transfected with JP-45–pFP-N3–DsRed2 construct (A, n=17) or pFP-N3/DsRed2 vector alone as control (B, n=15). As the magnitude of JP-45–DsRed2 fluorescence increased, the peak charge-movement significantly decreased (Fig. 7A), a phenomenon that was not observed in the control cells transfected only with the pFP-3/DsRed2 plasmid (Fig. 7B). For analysis of the charge-movement versus membrane-voltage relationship of cells transfected with either JP-45–pFP-

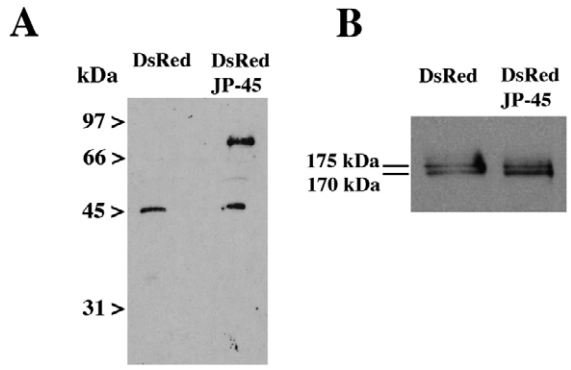

Fig. 6. Overexpression of JP-45 in C2C12 cells does not affect the expression levels of the $Ca_v1.1$ subunit. C2C12 cells were transfected either with the pFP-N3–DsRed2–JP-45 vector or with pFP-N3–DsRed2 alone as control. (A) Microsomes were prepared from transfected differentiated C2C12; 5 μg protein were separated on a 10% SDS-PAGE, blotted onto nitrocellulose and probed with anti-JP-45 polyclonal Ab, followed by HR-coupled protein G. The immunoreactive band was visualized by chemiluminescence. Note that control cells show the endogenous JP-45 immunoreactive band alone, whereas cells transfected with pFP-N3–DsRed2–JP-45 show an additional band of approximately 70 kDa, representing the DsRed–JP-45 fusion protein. (B) Immunoprecipitation and western blot analysis of $Ca_v1.1$ subunit expression in C2C12 cells transfected with pFP-N3–DsRed2 or pFP-N3–DsRed2–JP-45. Results are representative of three different transfection experiments.

N3–DsRed2 (Fig. 7C) or pFP-N3–DsRed2 plasmid (Fig. 7D), data points were fitted to a Boltzmann equation of the form:

$$Q_{on} = Q_{max} / [1 + \exp(V_{Q1/2} - V_m)/K] ,$$

where Q_{max} is the maximum charge, V_m is the membrane potential, $V_{Q1/2}$ is the charge-movement half-activation potential and K is the steepness of the curve. When cells were pooled for the analysis, Q_{max} was significantly lower in JP-45/pFP-N3/DsRed2 transfected than in control cells, whereas $V_{Q1/2}$ was shifted to more negative potentials in the former group. The best fitting parameters for Q_{max}, $V_{Q1/2}$ and K recorded in both groups of cells are included in Table 1. No differences in the steepness of the curve were recorded. To better characterize the voltage-dependence of the charge movement, the group of cells transfected with JP-45–pFP-N3–DsRed2 (Fig. 7A,C) were separated into two subgroups, either exhibiting the five highest or lowest Q_{max} values (Fig. 7E). This approach allowed to identify a more obvious difference not only in Q_{max} (~threefold) but also in the half activation potential of the charge movement (Table 1). High expression levels of JP-45 are associated with a shift of $V_{Q1/2}$ to more negative potentials of ~10 mV (Fig. 7C,D). No differences in the steepness of the curve were observed between these two groups of cells (Table 1).

The observation that alteration of peak charge movement is tightly linked to the magnitude of JP-45 expression suggests that, the stoichiometry of the JP-45/$Ca_v1.1$ supramolecular complex is crucial for the proper function of the $Ca_v1.1$. If this is so, we reasoned that depletion of JP-45 in differentiated myotubes would similarly affect the charge movement of $Ca_v1.1$.

Effect of JP-45 gene silencing on $Ca_v1.1$ function

The mRNA encoding JP-45 was much less abundant in C2C12 myotubes transfected with the plasmid containing JP-45 siRNA than in cells transfected with the control pSHAG vector (Fig. 8A). The presence of residual mRNA for JP-45 could either be due to the presence of a small subpopulation of cells which had not been transfected with the JP-45 siRNA construct, or to the inability of the construct to fully eliminate the transcript of JP-45. The amount of β-actin transcript did not differ significantly between cells transfected with the two constructs (Fig. 8A lower panel). Western blot analysis was performed to confirm depletion of JP-45 in differentiated C2C12 myotubes. Expression of JP-45 in C2C12 cells transfected with JP-45 siRNA is lower than the detection limit of the anti-JP-45 Abs that were

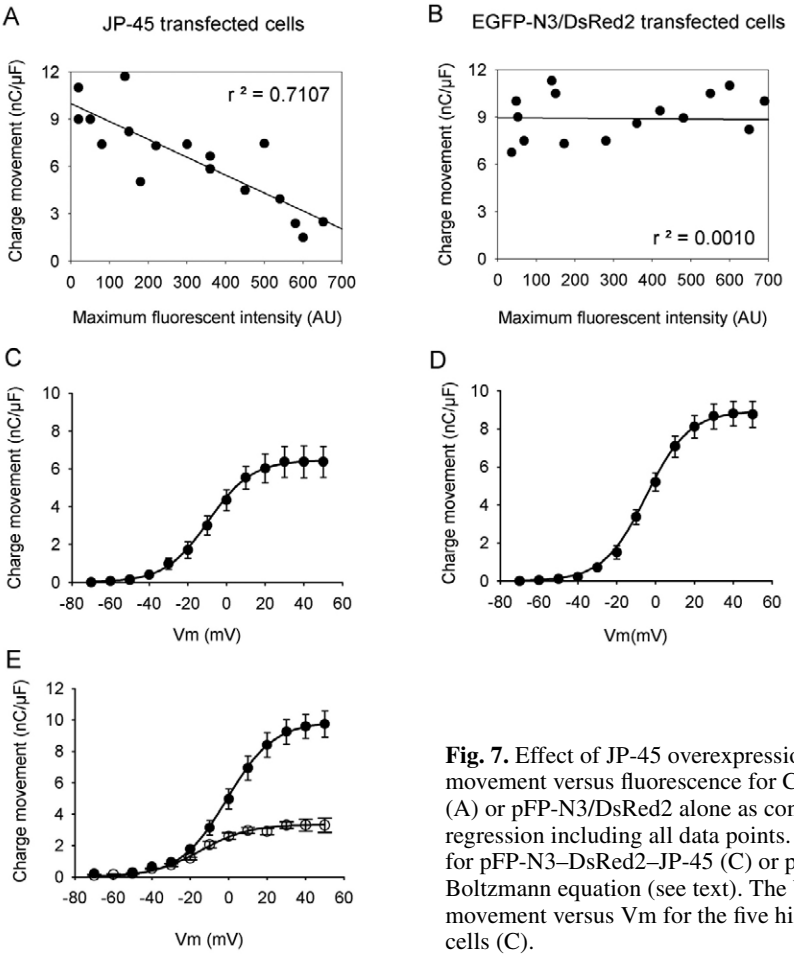

Fig. 7. Effect of JP-45 overexpression on $Ca_v1.1$ charge movement. (A,B) Maximum charge-movement versus fluorescence for C2C12 cells transfected with either pFP-N3–DsRed2 JP-45 (A) or pFP-N3/DsRed2 alone as control (B). The lines in A and B represent the linear regression including all data points. (C,D) Charge-movement versus membrane-voltage (Vm) for pFP-N3–DsRed2–JP-45 (C) or pFP-N3–DsRed2 plasmid (D) transfected cells fitted to a Boltzmann equation (see text). The best fitting parameters are included in Table 1. (E) Charge-movement versus Vm for the five highest and lowest Q_{max} values (E) from JP-45 transfected cells (C).

Table 1. Best-fitting parameters describing the voltage-dependence of charge movement in JP-45-overexpressing C2C12 myotubes

	Best-fitting parameters		
	Q_{max} (nC μF^{-1})	$V_{Q1/2}$ (mV)	K
JP-45-transfected cells (n=17)	6.4±0.3	–9.1±1.2	11.4±1.5
Control-transfected cells (vector only) (n=15)	8.9±0.3 (**)	–5.1±0.7 (**)	10.7±1.1 (n.s.)
JP-45; max Q-values (n=5)	10.1±1.0	–3.2±0.03	12.5±0.6
JP-45; min Q-values (n=5)	3.2±0.04 (**)	–14.5±0.13 (**)	12.5±0.5 (n.s.)

Best-fitting parameters for cells transfected with JP-45 or vector only, and of maximum (Max) and minimum (Min) charge-movement values (Q) for JP-45. **P<0.05; n, number of cells. n.s., not significant. Values are the mean ± s.e.m.

Table 2. Best-fitting parameters describing the voltage-dependence of charge movement in C2C12 myotubes transfected with JP-45 siRNA or pSHAG

	Best-fitting parameters		
	Q_{max} (nC μF^{-1})	$V_{Q1/2}$ (mV)	K
JP-45 siRNA (n=18)	5.8±0.37	–2.1±0.03	12.9±0.6
pSHAG vector (n=17)	8.7±0.41(*)	–3.2±0.04	13.0±0.7

Values are the mean ± s.e.m.; n, number of cells; *P<0.05.

raised against the N-terminal-interacting domain of the protein (Fig. 8B). However, we did not see changes in the expression of the housekeeping gene β-actin. Having established a reduction in transcription and expression of JP-45, we next measured $Ca_v1.1$ charge-movement. C2C12 cells were co-transfected with pFP-N3–DsRed2 and either the JP-45 siRNA pSHAG vector or pSHAG vector. Based on the expression of the DsRed2 reporter, C2C12 cells were identified and charge-movement measurements were performed. Fig. 9A shows that depletion of JP-45 in C2C12 myotubes is associated with a decrease in Q_{max}, apparently without affecting $V_{Q1/2}$ or the steepness of the curves (Table 2). Fig. 9 also shows charge-movement traces recorded in C2C12 cells transfected with pSHAG (B) or JP-45 siRNA (C). The lower Q_{max} value in JP-45-depleted C2C12 cells might originate from a decrease in the amount of $Ca_v1.1$ in muscle cell membrane. To verify this, we quantified by western blot analysis the relative amount of the $Ca_v1.1$ in membranes of C2C12 cells that had been transfected with JP-45 siRNA or pSHAG. The $Ca_v1.1$ shows two distinct high-molecular mass bands of 175 kDa and 170 kDa (Fig.9 D,E) (Leung et al., 1987). Furthermore, in JP-45-depleted C2C12 myotubes, there is a significant reduction of the immunoreactive band that referes to the $Ca_v1.1$ (Fig. 9D,E). Expression of the $Ca_v1.1$, measured as the ratio of the immunopositive band between siRNA-JP-45-transfected and control pSHAG-vector-transfected C2C12 cells, was 0.63±0.10 (mean ± s.e.m., n=4). The fractional decrease of $Ca_v1.1$ expression is 0.37±0.09 (mean ± s.e.m., n=4) and matches the decrease in charge movement (fractional decrease is 0.34) shown in Table 2. These results indicate that JP-45 is important for proper insertion of the α1.1 subunit into the membrane of muscle cells.

A number of data have been obtained in the last few years concerning structural determinant(s) necessary for the proper functional insertion of $Ca_v1.1$ into the plasma membrane. Although not all aspects of the functional insertion into the membrane and of the targeting of the $Ca_v1.1$ are fully understood, the emerging idea is that cooperation of the AID domain in the I-II loop with the C-terminal domain, as well as

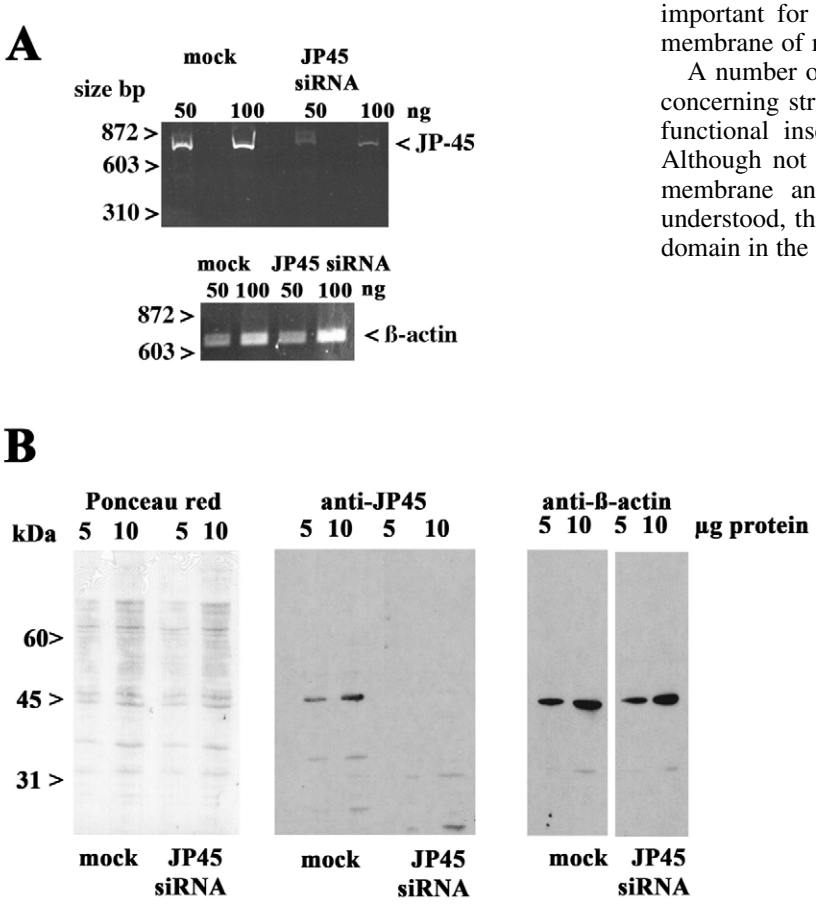

Fig. 8. JP-45 gene silencing in differentiated C2C12 myotubes. (A) Total RNA was extracted from transfected and differentiated C2C12 cells and converted into cDNA. The cDNA encoding JP-45 and β-actin was amplified by PCR. Amplified DNA obtained from 50 ng or 100 ng RNA was separated on a 7.5% acrylamide gel (JP-45, top panel) or a 1% agarose gel (β-actin, bottom panel). (B) Microsomal proteins from transfected and differentaiated C2C12 cells were prepared, separated on a 10% SDS-PAGE, blotted onto nitrocellulose and probed with anti-JP-45 Abs (central panel) or commercial anti-β-actin Abs, followed by peroxidase-labelled secondary Abs. Immunoreactive bands were visualized by chemiluminescence. Panel on the right shows blotted proteins stained with Ponceau Red. Results are representative of experiments carried in three different transfection experiments.

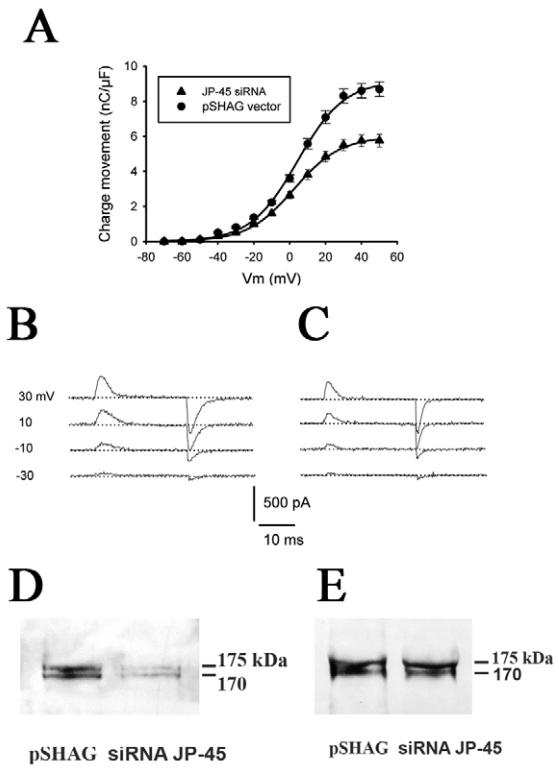

Fig. 9. JP-45 gene silencing modifies $Ca_v1.1$ charge movement. Charge-movement versus membrane-voltage (Vm) recorded in C2C12 cells transfected with JP-45 siRNA (n=18). Control cells were transfected with pSHAG vector (n=17). (A) Data points, expressed as mean ± s.e.m., were fitted to a Boltzmann equation (see text). Best fitting parameters are shown in Table 2. (B,C) Charge-movement records in the –30 mV to +30 mV range. Numbers on the left indicate the membrane potential. Dotted lines represent the baseline. (D,E) Immunoprecipitation and western blot analysis of $Ca_v1.1$ expression in C2C12 cells transfected with siRNA JP-45 and control pSHAG vector. Two assays from a total of four. The $Ca_v1.1$ expression in D and E decreased by 69% and 28%, respectively. The location of the molecular mass standards in kDa are depicted on the right.

the tertiary and quaternary structure assembly of the Ca_v1 complex, play a crucial role in the functional expression of the $Ca_v1.1$ in the cell membrane (Flucher et al., 2002). However, involvement of additional protein-protein interactions between other polypeptides of the triad membrane has been implied for the proper functional insertion of the $Ca_v1.1$. We suggest that JP-45 is one of these additional polypeptides important for the proper assembly of the $Ca_v1.1$ macromolecular complex into the plasma membrane.

Here, we have shown that JP-45 domain 2 interacts with the AID sequence and with the C-terminal domain of the $Ca_v1.1$, two important structural determinants for functional expression of the $Ca_v1.1$. In addition, we have provided clear evidence that the level of JP-45 expression in C2C12 myotubes affects the functional properties and expression of $Ca_v1.1$. By altering expression levels of JP-45 in differentiated C2C12 myotubes by overexpressing its cDNA or by JP-45 gene silencing, the stoichiometry of the JP-45–$Ca_v1.1$ supramolecular complex is dramatically altered. It is tempting to speculate that alteration of the stoichiometry of the complex influences the functional expression of the $Ca_v1.1$ by different mechanisms. Fig. 10 summarizes a speculative model, which describes the potential mode of action of JP-45 on $Ca_v1.1$ function and underlines the importance of the correct stoichiometry of JP-45–$Ca_v1.1$ on the functional expression of $Ca_v1.1$. Overexpression of JP-45 does not seem to induce major changes in the expression levels of α1.1, however it could enforce occupation of its binding site of the I-II loop. This occupation of the JP-45 binding site within the I-II loop might occur as consequence of a partial dissociation of the Ca_v1 β1a subunit or through interaction with the $Ca_v1.1$, which does not stably bind β1a subunit (Garcia et al., 2002; Jones et al., 2002). The I-II loop is adjacent to a repeat within the α1.1 subunit domain involved in channel gating. It is tempting to speculate that the effect of the overexpression and binding of JP-45 to the binding site within I-II loop is twofold: (1) Interference with the β1a action on gating currents (Strube et al., 1996, Sheridan et al., 2003). (2) Perturbation of the functional role of the adjacent repeat on channel function. Each outcome, or the combination of both, would confer a restricted conformation on the JP-45–$Ca_v1.1$ supramolecular complex,

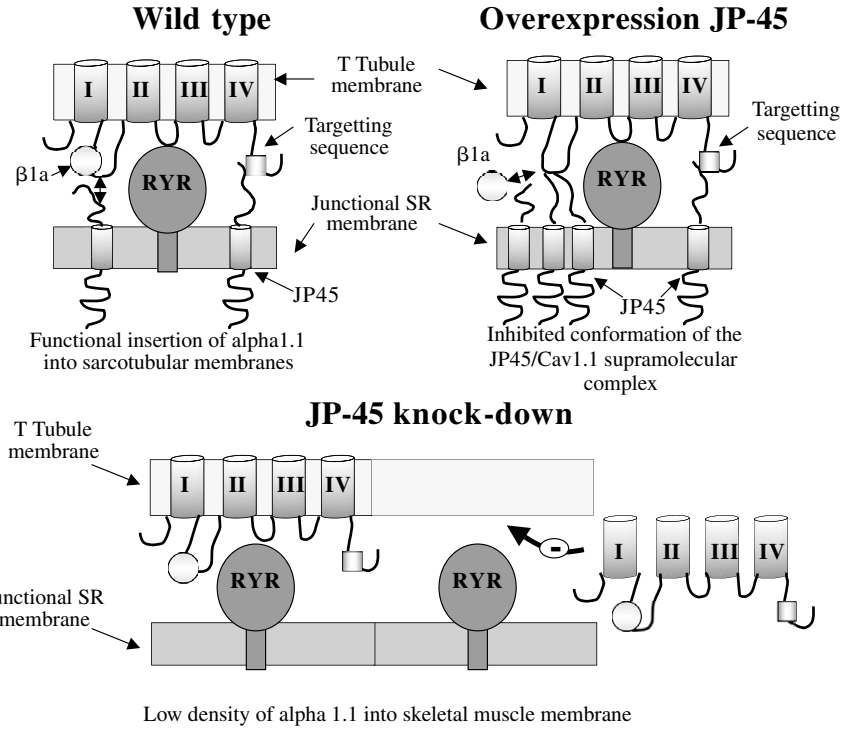

Fig. 10. Model depicting the potential functional role of JP-45.

leading to a decrease in charge movement. However, as indicated by western blot analysis, depletion of JP-45 affects the total amount of $Ca_v1.1$ in the cell membrane and, in parallel, also decreases the maximal charge movement. The mechanism leading to the decrease in the amount of $Ca_v1.1$ in cell membranes of JP-45-depleted cells might have several explanations. First, our results show that JP-45 interacts with the C-terminal domain, a region that has been shown to encompass a sequence involved in membrane targeting. When this sequence does not interact with JP-45, proper membrane targeting of $Ca_v1.1$ might be impaired. Second, JP-45 is involved in stabilizing the Ca_v1 complex. The functional consequence of both events is a decrease in Q_{max}, with no changes in the voltage dependence of the charge movement.

JP-45 is expressed at a very early stage of skeletal-muscle development – its transcript appears in 15-day-old embryos (Anderson et al., 2003) – in a developmental phase in which ER-SR membrane transition is not completed. In immature skeletal muscle fibres JP-45 might be localized in the ER-SR membrane network; then, in adult muscle fibres, JP-45 is targeted to the junctional face membrane of the SR. JP-45 might be involved in the retention of the $Ca_v1.1$ into the ER-SR membrane during the assembly of the $Ca_v1.1$ complex at an early stage of skeletal-muscle development. The appearance of the β1a subunit interferes with the interaction of JP-45 with the I-II loop of the $Ca_v1.1$. Such an event, together with an interaction of JP-45 and the C-terminal targeting domain, allows the functional expression of the $Ca_v1.1$ to the transverse tubular membranes.

Materials and Methods

Experimental procedures

pGex plasmids, nitrocellulose, rainbow molecular weight markers, glutathione-Sepharose, and [^{32}P]dCTP were from Amersham Biosciences; goat anti-α1 subunit polyclonal Abs against the skeletal muscle $Ca_v1.1$ were from Santa Cruz Biotechnology Inc.; isopropyl-β-D-thiogalactoside (IPTG), chemiluminescence kit, restriction enzymes, fugene transfection reagent, peroxidase-conjugated anti-goat Abs and EDTA-free anti-protease cocktail were from Roche Applied Science; protein-G peroxidase, protein assay determination kit and SDS-PAGE protein standards were from Bio-Rad; Talon metal affinity resin was from BD Bioscience; tricine, anti-poly-histidine, anti-β-actin Abs and peroxidase-conjugated anti-mouse Abs were from Sigma. Jet PEI transfection reagent was from Polyplus-Transfection SAS (Illkirch, France). Protein G plus Agarose was from Santa Cruz Biotechnology, Santa Cruz, CA. The pFP-N3/DsRed2 vector was constructed by in-frame substitution of the sequence encoding EGFP with that of DsRed2 in the pEGFP plasmid (Clonetech). The sequence of the plasmid backbone used for subsequent cloning of JP-45 cDNA was confirmed by sequencing. All other chemicals were reagents of highest grade available.

Production and purification of fusion proteins

PCR-amplified cDNA encoding overlapping sequences of mouse skeletal muscle JP-45 were cloned in-frame into the multiple cloning site of pGex5x-3. PCR amplification conditions and primer sequences were as previously described (Anderson et al., 2003), using the following sets of primers (forward and reverse, respectively): domain 1, encompassing residues 1-29 (5′-AGAATTCTATGACTACCAGAGGCCTGG-3′ and 5′-AGTCGACGGCTGGTCCCTCCAGAAAT-3′); domain 2, encompassing residues 1-80 (5′-AGAATTCTATGACTACCAGAGGCCTGG-3′ and 5′-AGTCGACTGTGCTCTCCTTGCCCGCTA-3′); domain 3, encompassing residues 81-125 (5′-AGAATTCTGGCAAAGCGGGAACAA-3′ and 5′-AGTCGACATCTCCCCAGGGCAGGTC-3′); the N-terminus, encompassing residues 1-125 (5′-AGAATTCTATGACTACCAGAGGCCTGG-3′ and 5′-AGTCGACATCTCCCCAGGGCAGGTC-3′); the C-terminus, encompassing residues 149-331 (5′-AGAATTCTCGGGACGCAGTGGCT-3′ and 5′-AGTCGACGTCACGCCCCTTCCCTCGCTT-3′). The *EcoR*I restriction site was added to facilitate subsequent subcloning. cDNA was amplified in a Perkin Elmer GeneAmp 2400 PCR System under the following conditions: 5 minutes at 95°C, followed by 35 cycles of 40 seconds annealing at 61°C, 45 seconds extension at 72°C, 30 seconds denaturation at 92°C and a final elongation step of 4 minutes at 72°C.

The cDNAs encoding different domains of rabbit skeletal muscle $Ca_v1.1$ α1.1 subunit (Tanabe et al., 1987) were cloned into the pMR78 expression vector designed to express His-tagged proteins. The α1.1 subunit constructs used include the N-terminus (encompassing residues 1-51), the I-II loop (encompassing residues 335-432), the II-III loop (encompassing residues 654-797), the III-IV loop (encompassing residues 1059-1118), the proximal C-terminus (encompassing residues 1382-1585), the distal C-terminus (encompassing residues 1588-1878) and the full-length $Ca_v1.1$ β1a subunit. All constructs were checked by direct sequencing. Plasmids were used to transform *E.coli* DH5α cells and fusion-protein production was induced by the addition of 100 μM of isopropyl-β-D-thiogalactoside (IPTG). Fusion proteins were purified, according to the manufacturer's recommendations, with glutathione-Sepharose for GST-tagged fusion proteins and the Talon metal affinity resins for the His-tagged α1.1 subunit fusion proteins. The protein concentration of the purified proteins was determined with the Bio-Rad protein assay kit and bovine serum albumin as standard (Bradford, 1976). Proteins eluted from the affinity columns were analysed by SDS-PAGE or Tricine-SDS-PAGE (Schagger and von Jagow, 1987) and visualized by either Coomassie Brilliant Blue or stained with anti-poly-histidine Abs.

Immunoprecipitation and co-immunoprecipitation experiments

Light microsomal vesicles derived from rabbit skeletal muscle were prepared as described by Saito et al. (Saito et al., 1984) Membranes were solubilized at a final concentration of 1 mg/ml, for 30 minutes at room temperature in a buffer composed of 1% CHAPS, 200 mM NaCl, 1 mM dithiothreitol, 50 mM Tris-HCl pH 8.5 to which the protease inhibitor cocktail was added. Co-immunoprecipitation experiments of native proteins were performed as previously described with the monoclonal anti-JP-45 Ab (Anderson et al., 2003). To identify the domain(s) of JP-45 interacting with the $Ca_v1.1$, CHAPS-solubilized light microsomal vesicles were incubated for 60 minutes with glutathione-Sepharose beads to which GST-JP-45 fusion proteins had been bound. Following low-speed centrifugation, the beads were washed three times with PBS; bound proteins were eluted using glutathione elution buffer, separated on a 10% SDS-PAGE and transferred onto nitrocellulose. To identify JP-45-binding domains of $Ca_v1.1$, the JP-45 domain-2 fusion protein encompassing was immobilized on GST-Sepharose beads and incubated for 60 minutes with purified His-tagged fusion proteins covering various domains of the α1.1 subunit, including the N-terminal domain, the I-II, II-III, III-IV loops, the C-terminal-distal and C-terminal-proximal domains, and the β1a domain in 10 mM HEPES and 150 mM NaCl plus anti-proteases. Beads were processed as described above.

C2C12 cells were washed with PBS, treated with 1% digitonin buffer (1% digitonin, 185 mM KCl, 1.5 mM $CaCl_2$, 10 mM HEPES pH 7.4) on ice for 1 hour and centrifuged at 10,000 ***g*** for 10 minutes at 4°C. The lysate (500 μg total protein) was precleared by adding 0.5 μg of mouse IgG together with 20 μl of Protein G plus Agarose, and incubated for 30 minutes on a rotating device at 4°C. After centrifugation at 1000 ***g***, the supernatant was transferred to a fresh tube on ice. Mouse $Ca_v1.1$ α1 subunit primary Ab (IIF7) (kindly provided by Kevin P. Campbell, University of Iowa, Howard Hughes Medical Institute, Iowa City, IA) (Leung et al., 1987) was added and incubated overnight at 4°C. Then 20 μl Protein G plus Agarose was added to each tube and incubated for 2 hours. After centrifugation, the pellets were washed with PBS and resuspended in 20 μl of double-strength sample buffer for 30 minutes at room temperature (Murray and Olendieck, 1997). The proteins were separated on a 10% SDS-PAGE gel and subsequently transferred onto PVDF membrane. Non-specific binding was blocked by incubating the membrane in 5% non-fat milk in PBS for 60 minutes at room temperature. Incubation in the primary Ab (1:1000 diluted in blot buffer) was for 2 hours at room temperature after which proteins were washed three times for 5 minutes with PBS. The membrane was incubated with anti-mouse IgG conjugated with horseradish peroxidase (HP) for 60 minutes, washed, and finally incubated in ECL Reagent and visualized in X-ray films. Autoradiograms were scanned and analyzed with KODAK-1D Image Analysis Software (Eastman Kodak Company, Rochester, NY).

Polyclonal Ab production and western blot analysis

Rabbit polyclonal antiserum was generated by immunizing a New Zealand white rabbit with glutathione-Sepharose purified GST-JP-45 fusion protein encompassing the cytoplasmic domain (aa 1-125) of JP-45. Serum was tested for the presence of Ab one month after immunization and subsequently the IgG fraction was purified by protein A column chromatography. Immunodetection of α1.1 subunit His-tagged fusion proteins was carried out with monoclonal anti-poly-histidine Ab, followed by HP-conjugated anti-mouse IgG; immunodetection of α1.1 subunit and JP-45 was carried out as described (Anderson et al., 2003). Immunopositive bands were visualized by chemiluminescence.

Cell culture and transfection

The mouse C2C12 muscle cell line was obtained from American Type Culture Collection (ATCC, Rockville, MD), cultured in standard conditions and maintained in growth medium (Dulbecco's modified Eagle's medium, DMEM, supplemented with 20% foetal bovine serum, 100 units/ml penicillin and 100 μg/ml streptomycin). Cells were induced to differentiate by switching the medium to differentiation

medium (DMEM supplemented with 2% horse serum, 100 units/ml penicillin and 100 μg/ml streptomycin). For overexpression experiments, C2C12 cells were transfected with the cDNA encoding JP-45, cloned in-frame into a hybrid pFP-N3–DsRed2 vector. Briefly, 2 days after plating, cells were transfected by adding a solution of plasmid DNA (1 μg) and 3 μl FUGENE6 previously mixed for 30 minutes at room temperature, to the tissue culture medium. Electrophysiological measurements were made on differentiated cells 5-6 days after cell transfection. To deplete C2C12 of JP-45, we transfected cells with a JP-45 siRNA vector pSHAG. JP-45 RNA interference oligos were designed with siRNA Wizard software available at InvivoGene webpage. We chose the GCTCAACAAGTGCCTGG-TACTGGCCTCGCTG nucleotides of JP-45 coding sequence. Complementary JP-45 RNAi oligos were synthesised according to the instructions of G. Hannon (Cold Spring Harbor), annealed and ligated downstream U6 RNA Pol III promoter of the pSHAG-1 vector as previously described (Treves et al., 2004). The nucleotide sequence of the JP-45 siRNA construct was verified by sequencing. For transfection experiments, C2C12 cells were plated on 12-mm diameter glass coverslips or on 100-mm diameter tissue culture dishes and once they reached 50-60% confluency they were transfected by a combination of CaPO4 and Jet PEI, using a total of 7.5 μg of plasmid DNA (coverslips) or 15 μg plasmid DNA (cell culture dishes). The day after transfection, the medium was changed and the cells were allowed to recover for 24 hours. On day 3, the cells were induced to differentiate by switching the medium to differentiation medium (DMEM supplemented with 2% horse serum, 100 units/ml penicillin and 100 μg/ml streptomycin) and were transfected again as described above to increase transfection efficiency. The next day fresh differentiation medium was added and cells were allowed to differentiate for another 3 days, after which multinucleated myotubes were clearly visible. Total RNA was extracted from transfected cells, converted into DNA as previously described (Treves et al., 2004) and reverse transcriptase (RT)-PCR was carried out with JP-45-specific or β-actin-specific primers. Western bloting was done with an Ab recognizing the N-terminal domain of JP-45.

Charge movement and fluorescence recordings

For charge movement recordings, C2C12 cells were plated on glass coverslips and mounted in a small flow-through Lucite chamber positioned on a microscope stage. Myotubes were continuously perfused with the external solution (see below) using a push-pull syringe pump (WPI, Saratoga, FL.). Cells were voltage-clamped in the whole-cell configuration of the patch-clamp (Hamill et al., 1981; Wang et al., 1999) using an Axopatch-200B amplifier (Axon Instruments/Molecular Devices, Union City, CA). Micropipettes were pulled from borosilicate glasses (Boralex) using a Flaming Brown micropipette puller (P97, Sutter Instrument Co., Novato, CA) to obtain electrode resistance ranging from 2-4 MΩ. The composition of the internal solution (pipette) was (in mM): 140 Cs-aspartate; 5 Mg-aspartate$_2$, 10 Cs_2EGTA (ethylene glycol-bis(α-aminoethyl ether)-N,N,N′N′-tetraacetic acid), 10 HEPES, pH was adjusted to 7.4 with CsOH. The high concentration of Mg^{2+} in the pipette solution helped to stabilize the preparation for longer periods. The external solution contained (in mM): 145 TEA (tetraethylammonium)-Cl, 10 $CaCl_2$, 10 HEPES and 0.001 tetrodotoxin. Solution pH was adjusted to 7.4 with TEA.OH. For charge movement recording, Ca^{2+} current was blocked by the addition of 0.5 Cd^{2+} plus 0.3 La^{3+} to the external solution (Hamill et al., 1981; Wang et al., 1999; Wang et al., 2000; Beam and Franzini-Armstrong, 1997).

Whole-cell currents were acquired and filtered at 5 kHz with pClamp 6.04 software (Axon). A Digidata 1200 interface (Axon) was used for A-D conversion. Membrane current during a voltage pulse, P, was initially corrected by analogue subtraction of linear components. The remaining linear components were digitally subtracted on-line using hyperpolarizing control pulses of one-quarter test pulse amplitude (–P/4 procedure) (Delbono, 1992). The four control pulses were applied before the test pulse. We recorded the charge movement corresponding to gating of the L-type Ca^{2+} channel $Ca_v1.1$. To this end, we used a prepulse protocol consisting of a 2-second prepulse to –30 mV and a subsequent 5-millisecond repolarization to a pedestal potential of –50 mV, followed by a 12.5-millisecond depolarization from –50 mV to 50 mV with 10-mV intervals (Adams et al., 1990). The optimal duration of the prepulse defined as the value at which no further immobilization of charge movement is attained was determined to be 2 seconds, after testing a range of prepulses from 1-6 seconds (Wang et al., 2000). Intramembrane charge movements were calculated as the integral of the current in response to depolarizing pulses (charge on, Q_{on}) and were expressed per membrane capacitance (Coulombs per Farad). The complete blockade of the inward Ca^{2+} current was verified by the $Q_{on} - Q_{off}$ linear relationship. Membrane capacitance was calculated as the integral of the transient current in response to a brief hyperpolarizing pulse from –80 mV (holding potential) to –100 mV.

To correlate the level of transfection with charge movement, we recorded fluorescence intensity arising from pFP-N3–DsRed2 in JP-45-transfected or pFP-N3–DsRed2-transfected cells with a Radiance 2100K1 laser scanning confocal system (Zeiss, Oberkochen, Germany). Fluorescence intensity was acquired in all the areas of the cell by using a krypton laser at 568 nm and recording the emission at 640 nm. The acquisition settings, including iris aperture (used at maximum), laser intensity, exposure, and gain were maintained unmodified from cell to cell to standardize recordings and make the comparison among cells valid. The maximum fluorescent intensity of the whole cell was analyzed in digitized images and expressed in arbitrary units (AU).

Data were analyzed using Student's *t*-test or analysis of variance (ANOVA). A value of $P<0.05$ was considered significant. Data are expressed as mean ± s.e.m. with the number of observations (*n*).

This work was supported by grants from the Schweizereische Stiftung für die Erforschung der Muskelkrankheiten, the Association Française contre les Myopathies, the European Union (Number HPRN-CT-2002-00331) and F.I.R.BRBAUO1ERMX, PRIN05, the Department of Anaesthesia, University Hospital Basel and by grants AG18755, AG13934 and AG15820 from the National Institute of Health/National Institute on Aging, USA.

References

Adams, B. A., Tanabe, T., Mikami, A., Numa, S. and Beam, K. G. (1990). Intramembrane charge movement restored in dysgenic skeletal muscle by injection of dihydropyridine receptor. *Nature* **346**, 569-572.

Ahern, C. A., Sheridan, D. C., Cheng, W., Mortenson, L., Nataaraj, P., Allen, P., DeWaard, M. and Coronado, R. (2003). Ca2+ current and charge movements in skeletal myotubes promoted by the beta-subunit of the dihydropyridine receptor in the absence of ryanodine receptor type 1. *Biophys. J.* **84**, 942-959.

Anderson, A. A., Treves, S., Biral, D., Betto, R., Sandona, D., Ronjat, M. and Zorzato, F. (2003). The novel skeletal muscle sarcoplasmic reticulum JP-45 protein. Molecular cloning, tissue distribution, developmental expression, and interaction with alpha 1.1 subunit of the voltage-gated calcium channel. *J. Biol. Chem.* **278**, 39987-39992.

Beam, K. G. and Franzini-Armstrong, C. (1997). Functional and structural approaches to the study of excitation-contraction coupling. *Methods Cell Biol.* **52**, 283-306.

Beurg, M., Ahern, C. A., Vallejo, P., Conklin, M. W., Powers, P. A., Gregg, R. G. and Coronado, R. (1999). Involvement of the carboxy-terminus region of the dihydropyridine receptor beta1a subunit in excitation-contraction coupling of skeletal muscle. *Biophys. J.* **77**, 2953-2967.

Bichet, D., Cornet, V., Geib, S., Carlier, E., Volsen, S., Hoshi, T., Mori, Y. and DeWaard, M. (2000). The I-II loop of the Ca2+ channel alpha1 subunit contains an endoplasmic reticulum retention signal antagonized by the beta subunit. *Neuron* **25**, 177-190.

Birnbaumer, L., Qin, N., Olcese, R., Tareilus, E., Platano, D., Costantin, J. and Stefani, E. (1998). Structures and functions of calcium channel beta subunits. *J. Bioenerg. Biomembr.* **30**, 357-375.

Bradford, M. M. (1976). A rapid and sensitive method for the quantitation of microgram quantities of protein utilizing the principle of protein-dye binding. *Anal. Biochem.* **72**, 248-254.

Catterall, W. A. (1995). Structure and function of voltage-gated ion channels. *Annu. Rev. Biochem.* **64**, 493-531.

Chen, Y., Li, M., Zhang, Y., He, L., Yamada, Y., Fitzmaurice, A., Shen, Y., Zhang, H., Tong, L. and Yang, J. (2004). Structural basis of the alpha1-beta subunit interaction of voltage-gated Ca2+ channels. *Nature* **429**, 675-680.

Chien, A. J., Zhao, X., Shirokov, R. E., Puri, T. S., Chang, C. F., Sun, D., Rios, E. and Hosey, M. M. (1995). Roles of a membrane-localized beta subunit in the formation and targeting of functional L-type Ca2+ channels. *J. Biol. Chem.* **270**, 30036-30044.

Costello, B., Chadwick, C., Saito, A., Chu, A., Maurer, A. and Fleischer, S. (1986). Characterization of the junctional face membrane from terminal cisternae of sarcoplasmic reticulum. *J. Cell Biol.* **103**, 741-753.

Delbono, O. (1992). Calcium current activation and charge movement in denervated mammalian skeletal muscle fibres. *J. Physiol. Lond.* **451**, 187-203.

Endo, M. (1977). Calcium release from sarcoplasmic reticulum. *Physiol. Rev.* **57**, 71-108.

Fleischer, S. and Inui, M. (1989). Biochemistry and biophysics of excitation-contraction coupling. *Annu. Rev. Biophys. Biophys. Chem.* **18**, 333-364.

Flucher, B. E., Kasielk, N. and Grabner, M. (2000). The triad targeting signal of the skeletal muscle calcium channel is localized in the COOH terminus of the alpha(1S) subunit. *J. Cell Biol.* **151**, 467-478.

Flucher, B. E., Weiss, R. G. and Grabner, M. (2002). Cooperation of two-domain Ca(2+) channel fragments in triad targeting and restoration of excitation- contraction coupling in skeletal muscle. *Proc. Natl. Acad. Sci. USA* **99**, 10167-10172.

Franzini-Armstrong, C. (1980). Structure of sarcoplasmic reticulum. *Fed. Proc.* **39**, 2403-2409.

Franzini-Armstrong, C. A. and Jorgensen, A. O. (1994). Structure and development of E-C coupling units in skeletal muscle. *Annu. Rev. Physiol.* **56**, 509-534.

Garcia, R., Carrillo, E., Rebolledo, S., Garcia, M. C. and Sanchez, J. A. (2002). The beta1a subunit regulates the functional properties of adult frog and mouse L-type Ca2+ channels of skeletal muscle. *J. Physiol.* **545**, 407-419.

Grabner, M., Dirksen, R. T., Suda, N. and Beam, K. G. (1999). The II-III loop of the skeletal muscle dihydropyridine receptor is responsible for the Bi-directional coupling with the ryanodine receptor. *J. Biol. Chem.* **274**, 21913-21919.

Gregg, R. G., Meissing, A., Strube, C., Beurg, M., Moss, R., Behan, M., Sukhareva, M., Haynes, S., Powell, J. A., Coronado, R. et al. (1996). Absence of the beta subunit (cchb1) of the skeletal muscle dihydropyridine receptor alters expression of the alpha 1 subunit and eliminates excitation-contraction coupling. *Proc. Natl. Acad. Sci. USA* **93**, 13961-13966.

Hamill, O. P., Marty, A., Neher, E., Sakmann, B. and Sigworth, F. J. (1981). Improved

patch-clamp techniques for high-resolution current recording from cells and cell-free membrane patches. *Pflugers Arch.* **391**, 85-100.

Ito, K., Komazaki, S., Sasamoto, K., Yoshida, M., Nishi, M., Kitamura, K. and Takeshima, H. (2001). Deficiency of triad junction and contraction in mutant skeletal muscle lacking junctophilin type 1. *J. Cell Biol.* **154**, 1059-1067.

Kugler, G., Weiss, R. G., Flucher, B. E. and Grabner, M. (2004). Structural requirements of the dihydropyridine receptor alpha1S II-III loop for skeletal-type excitation-contraction coupling. *J. Biol. Chem.* **279**, 4721-4728.

Jones, L. P., Wei, A. K. and Yue, D. T. (1998). Mechanism of auxiliary subunit modulation of neuronal alpha1E calcium channels. *J. Gen. Physiol.* **112**, 125-143.

Jones, S. W. (2002). Calcium channels: when is a subunit not a subunit? *J. Physiol.* **545**, 33.

Lacerda, A. E., Kim, H. S., Ruth, P., Perez-Reyes, E., Flockerzi, V., Hofmann, F., Birnbaumer, L. and Brown, A. M. (1991). Normalization of current kinetics by interaction between the alpha 1 and beta subunits of the skeletal muscle dihydropyridine-sensitive Ca2+ channel. *Nature* **352**, 527-530.

Lamb, G. D. and Stephenson, D. G. (1990). Control of calcium release and the effect of ryanodine in skinned muscle fibres of the toad. *J. Physiol. Lond.* **423**, 519-542.

Leung, A. T., Imagawa, T. and Campbell, K. P. (1987). Structural characterization of the 1,4-dihydropyridine receptor of the voltage-dependent Ca2+ channel from rabbit skeletal muscle. Evidence for two distinct high molecular weight subunits. *J. Biol. Chem.* **262**, 7943-7946.

Ma, J. and Pan, Z. (2003). Junctional membrane structure and store operated calcium entry in muscle cells. *Front. Biosci.* **8**, d242-d255.

Meissner, G. (1994). Ryanodine receptor/Ca2+ release channels and their regulation by endogenous effectors. *Annu. Rev. Physiol.* **56**, 485-508.

Murray, B. E. and Ohlendieck, K. (1997). Cross-linking analysis of the ryanodine receptor and alpha1-dihydropyridine receptor in rabbit skeletal muscle triads. *Biochem. J.* **324**, 689-696.

Nakai, J., Sekiguchi, N., Rando, T. A., Allen, P. D. and Beam, K. G. (1998). Two regions of the ryanodine receptor involved in coupling with L-type Ca2+ channels. *J. Biol. Chem.* **273**, 13403-13406.

Pragnell, M., De Waard, M., Mori, Y., Tanabe, T., Snutch, T. P. and Campbell, K. P. (1994). Calcium channel beta-subunit binds to a conserved motif in the I-II cytoplasmic linker of the alpha 1-subunit. *Nature* **368**, 67-70.

Saito, A., Seiler, S., Chu, A. and Fleischer, S. (1984). Preparation and morphology of sarcoplasmic reticulum terminal cisternae from rabbit skeletal muscle. *J. Cell Biol.* **99**, 875-885.

Schagger, H. and von Jagow, G. (1987). Tricine-sodium dodecyl sulfate-polyacrylamide gel electrophoresis for the separation of proteins in the range from 1 to 100 kDa. *Anal. Biochem.* **166**, 368-379.

Sheridan, D. C., Cheng, W., Ahern, C. A., Mortenson, L., Alsammarae, D., Vallejo, P. and Coronado, R. (2003). Truncation of the carboxyl terminus of the dihydropyridine receptor beta1a subunit promotes Ca2+ dependent excitation-contraction coupling in skeletal myotubes. *Biophys. J.* **84**, 220-237.

Sheridan, D. C., Cheng, W., Carboneau, L., Ahern, C. A. and Coronado, R. (2004). Involvment of a heptad repeat in the carboxyl terminus of the dihydropyridine receptor beta1a subunit in the mechanism of excitation-contraction coupling in skeletal muscle. *Biophys. J.* **87**, 929-942.

Snutch, T. P. and Reiner, P. B. (1992). Ca2+ channels: diversity of form and function. *Curr. Opin. Neurobiol.* **2**, 247-253.

Strube, C., Beurg, M., Powers, P. A., Gregg, R. G. and Coronado, R. (1996). Reduced Ca2+ current, charge movement, and absence of Ca2+ transients in skeletal muscle deficient in dihydropyridine receptor beta 1 subunit. *Biophys. J.* **71**, 2531-2543.

Sutko, J. L. and Airey, J. A. (1996). Ryanodine receptor Ca2+ release channels: does diversity in form equal diversity in function? *Physiol. Rev.* **76**, 11027-11071.

Rios, E. and Pizarro, G. (1991). Voltage sensor of excitation-contraction coupling in skeletal muscle *Physiol. Rev.* **71**, 849-908.

Takeshima, H., Komazaki, S., Nishi, M., Iino, M. and Kangawa, K. (2000). Junctophilins: a novel family of junctional membrane complex proteins. *Mol. Cell* **6**, 11-22.

Tanabe, T., Takeshima, H., Mikami, A., Flockerzi, V., Takahashi, M., Kangawa, K., Kojima, M., Matsuo, H., Hirose, T. and Numa, S. (1987). Primary structure of the receptor for calcium channel blockers from skeletal muscle. *Nature* **328**, 313-318.

Treves, S., Franzini-Armstrong, C., Moccagatta, L., Arnoult, C., Grasso, C., Schrum, A., Ducreux, S., Zhu, M. X., Mikoshiba, K., Girard, T. et al. (2004). Junctate is a key element in calcium entry induced by activation of InsP3 receptors and/or calcium store depletion. *J. Cell Biol.* **166**, 537-548.

Tsien, R. W., Ellinor, P. T. and Horne, W. A. (1991). Molecular diversity of voltage-dependent Ca2+ channels. *Trends Pharmacol. Sci.* **12**, 349-354.

Van Petegem, F., Clark, K. A., Chatelain, F. C. and Minor, D. L., Jr (2004). Structure of a complex between a voltage-gated calcium channel beta-subunit and an alpha-subunit domain. *Nature* **429**, 671-675.

Wang, Z.-M., Messi, M. L. and Delbono, O. (1999). Patch-clamp recording of charge movement, Ca(2+) current, and Ca(2+) transients in adult skeletal muscle fibers. *Biophys. J.* **77**, 2709-2716.

Wang, Z.-M., Messi, M. L. and Delbono, O. (2000). L-Type Ca(2+) channel charge movement and intracellular Ca(2+) in skeletal muscle fibers from aging mice. *Biophys. J.* **78**, 1947-1954.

Zhang, L., Kelley, J., Schmeisser, G., Kobayashi, Y. M., Jones, L. R. (1997). Complex formation between junctin, triadin, calsequestrin, and the ryanodine receptor. Proteins of the cardiac junctional sarcoplasmic reticulum membrane. *J. Biol. Chem.* **272**, 23389-23397.

Zorzato, F., Anderson, A. A., Ohlendieck, K., Froemming, G., Guerrini, R. and Treves, S. (2000). Identification of a novel 45 kDa protein (JP-45) from rabbit sarcoplasmic-reticulum junctional-face membrane. *Biochem. J.* **351**, 537-543.

Journal of Cell Science